ACS chemical biology

Articles

pubs.acs.org/acschemicalbiology

# A Synthetic Peptide Mimic of λ-Cro shows Sequence-Specific Binding *in Vitro* and *in Vivo*

Abhishek Mazumder,[†] Atanu Maiti,[†] Koushik Roy, and Siddhartha Roy*

Divisions of Structural Biology and Bioinformatics, CSIR-Indian Institute of Chemical Biology, 4, Raja S.C. Mullick Road, Kolkata 700032, India

Supporting Information

**ABSTRACT:** Development of small synthetic transcription factors is important for future cellular engineering and therapeutics. This article describes the chemical synthesis of α-amino-isobutyric acid (Aib) substituted, conformationally constrained, helical peptide mimics of *Cro* protein from bacteriophage λ that encompasses the DNA recognition elements. The Aib substituted constrained helical peptide monomer shows a moderately reduced dissociation constant compared to the corresponding unsubstituted wild type peptide. A suitably cross-linked dimeric version of the peptide, mimicking the dimeric protein, recapitulates some of the important features of *Cro*. It binds to the operator site $O_R3$, a high affinity *Cro* binding site in the λ genome, with good affinity and single base-pair discrimination specificity. A dimeric version of an even shorter peptide mimic spanning only the recognition helix of the helix-turn-helix motif of the *Cro* protein was created following the same design principles. This dimeric peptide binds to $O_R3$ with affinity greater than that of the longer version. Chemical shift perturbation experiments show that the binding mode of this peptide dimer to the cognate operator site sequence is similar to the wild type *Cro* protein. A Green Fluorescent Protein based reporter assay *in vivo* reveals that the peptide dimer binds the operator site sequences with considerable selectivity and inhibits gene expression. Peptide mimics designed in this way may provide a future framework for creating effective synthetic transcription factors.

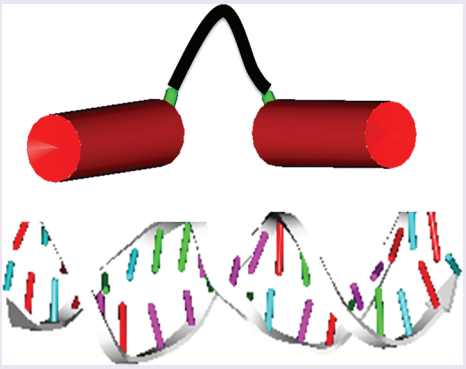

Design and synthesis of small or medium-sized molecules that can bind specifically to a given DNA sequence has been one of the important goals of chemical biology.[1,2] Significant efforts have been made toward designing molecules that bind DNA in a sequence-specific manner.[3−5] This is believed to be the first step toward design of synthetic transcription factors to regulate gene expression selectively. DNA-binding proteins, within polypeptide chain(s), have not only optimized sequence-specific binding but other functions such as target search and protein−protein interactions as well. A successful synthetic transcription factor should mimic all of these aspects.[6] The most straightforward way may be to explore peptide based mimics, where it may be possible to incorporate multiple features mentioned above by following principles learnt from extant DNA-binding proteins.

The helix, an important secondary structural element, has been widely used in nature in protein−protein and protein−DNA interactions. This is evidenced by a large number of helix containing DNA-binding motifs, *e.g.*, helix-turn-helix, zinc fingers, *etc.*[7−9] In many of these motifs, the major interaction points of the protein are sometimes confined to one recognition helix. In these cases, the rest of the protein behaves largely like a scaffold on to which the helix is grafted, imparting conformational constraint. The helix has also been the mainstay of many protein design studies.[10] Schepartz and colleagues have used an artificial scaffold to present a recognition helix that led to a successful mini transcription factor.[5] The work by the Schepartz group and involvement of helices in a large number of the DNA-binding proteins and localization of the interface mostly to the helices suggests that perhaps small helical peptide mimics can be synthesized to bind to the same sequence recognized by a DNA-binding protein, if several criteria are met. One of the critical issues is that a small peptide spanning the helix-turn-helix motif is likely to exist in a disordered structure in solution and hence would have to overcome the entropic disadvantage of a disorder−order transition (that is a random coil to helix transition) in order to bind the cognate DNA sequence. This unfavorable energetic cost will be most pronounced in cases where the parent transcription factor contains preformed recognition helices. Constraining short peptides in helical conformations could thus overcome this problem and form the basis for creating artificial gene regulatory proteins. This approach has already been taken with a side chain cross-linked peptide.[11] Due to protease resistance, the constrained peptide may also have enhanced stability, important for *in vivo* application.

α-Amino isobutyric acid (Aib) is a well-known alanine analogue that is known to strongly favor the helical conformation and can be incorporated in standard peptide

Received: December 14, 2011
Accepted: April 5, 2012
Published: April 5, 2012

  

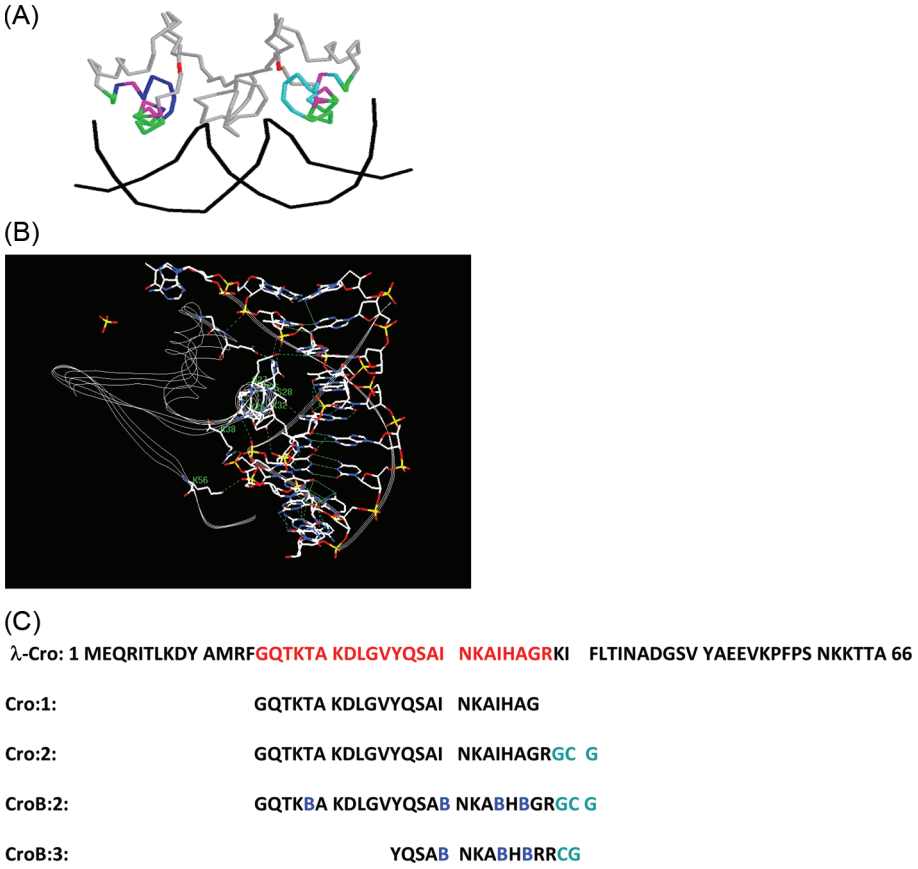


**Figure 1.** (A) Backbone representation of λ-Cro protein with its cognate operator (symmetric; PDB ID 4cro). Magenta represents the Aib positions, green represents the residues interacting with DNA, red represents the introduced cysteines, and the rest of the chain in Cro-1 is represented in cyan or blue (different subunits). (B) The hydrogen bonds between Cro and a synthetic operator are shown (green dashed line). The data was obtained from PDB ID 6cro. Both figures were generated using spdv. (C) Sequence alignment of different monomeric peptides with the parent Cro sequence. The residues marked in red in the Cro sequence are in the helix-turn-helix motif. The residues in blue are the Aib residues, and the residues in green are the non-Cro residues incorporated for dimer cross-linking.

synthesis protocols. Aib has important advantages as a helix inducer due to its strong preference for a Ramachandran angle in the helical range and can also be simply introduced in a solid-phase protocol without any additional step.[12] So, introduction of one or more Aib's may incline the peptide to a helical conformation overriding conformational preferences of other amino acid types present. The design and synthesis of such a constrained helical mimic would reduce the entropic cost involved in the transition from the disordered conformation of the wild type peptide to an ordered helical conformation required to bind the cognate DNA sequence, thus increasing the overall affinity of the mimic toward the cognate DNA.

*Cro* is a basic, dimeric protein consisting of 66 amino acid residues that plays an important part in the switch from lysogenic to lytic growth in phage λ.[13,14] The three-dimensional structure of this important protein has been solved both in the absence[15] and presence of cognate DNA.[16] This article reports a simple strategy for construction of a minimal *Cro* mimic with native-like specificity *in vitro*. The peptide mimic is also capable of blocking transcription *in vivo* with considerable selectivity.

## RESULTS AND DISCUSSION

**Design Strategy.** Many prokaryotic and phage DNA-binding proteins are symmetric dimers that recognize fully symmetric inverted repeat sequences or nearly symmetric ones. The binding energy is derived from sum of the two protein monomers binding to each half-site and the entropic advantage of two-headed binding, similar to the chelate effect. Although it is difficult to estimate how much entropic advantage of chelate-like effect contributes, it is likely to be significant.[17] The first step in creating a mimic as described above is to create a constrained peptide preserving the essential residues of the helix-turn-helix motif. The *Cro* protein from bacteriophage λ was chosen as the DNA−protein interface of this protein is largely confined to a relatively small section of the protein, *i.e.*, the recognition helix. The helix-turn-helix motif of λ-Cro spans residues 15−38,[15] and almost all of the interacting residues are present within this span (Figure 1A). The wild type peptide (Cro:1) containing no Aib substitutions was first synthesized (GQTKTAKDLGVYQSAINKAIHAG). To push the conformational equilibrium toward the helical conformation, α-amino-isobutyric acid (Aib) was introduced into the Cro:1 peptide in positions that are not part of the protein−DNA interface (Figure 1B). The substituted positions are T19, I30, I34, and A36 (CroB:1, GQTKBAKDLGVYQSABNKABHBG; incorporation of B in the name represents Aib substitution). Alignment of all of the monomeric sequences with appropriate highlights is presented in Figure 1C. The next step in the strategy to enhance binding is to link two recognition helices with a cross-linker of suitable length. For cross-linking purposes an additional 4 residues were added, which contains a cysteine near the C-terminus to create the CroB:2 peptide. If the Cro-


dx.doi.org/10.1021/cb200523n | *ACS Chem. Biol.* 2012, 7, 1084−1094

$O_R3$ crystal structure is used as a guide, the distance between the thiols of symmetry related cysteines will be about 11 Å. Hence, bis-maleimido hexane was chosen as the cross-linker, which spans around 16 Å. For further improvement of binding affinity, a smaller peptide mimic spanning only the recognition helix of the helix-turn-helix domain of the Cro protein was created (CroB:3). This shorter version of the peptide (lacking residues 15−25 of Cro) would lack a number of putative interactions with the backbone when compared to CroB:2 (*e.g.*, Q16 and T17) in the protein−DNA interface. The design of this shorter peptide also involves deletion of one residue and substitution of an additional arginine residue (for additional possible backbone interaction) to create the CroB:3 peptide. The cross-linking cysteine residues now correspond to position 39 instead of position 40 (Figure 1C). In the crystal structure, the C$\alpha$−C$\alpha$ distance is same for the 39−39 and 40−40 residues (approximately 16 Å). Sequence of all of the dimeric constructs are given in Methods section.

**Synthesis and Characterization of the Peptide Mimics.** The peptides were synthesized in a semiautomatic peptide synthesizer and purified by reverse phase HPLC. Masses of the peptides were confirmed by mass spectrometry (see Methods). Helical propensities of several of these peptides were also judged by circular dichroism spectroscopy. Figure 2

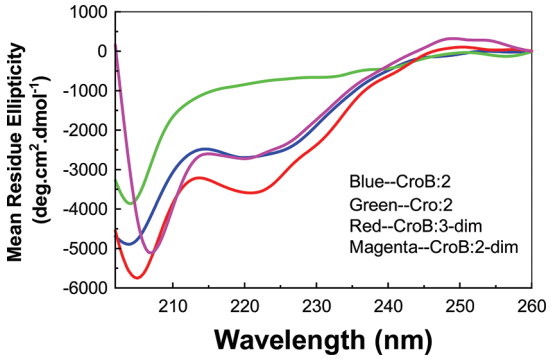


**Figure 2.** Overlay of the far UV circular dichroism spectra of Cro2 (no Aib), CroB:2, CroB:2-dim, and CroB:3-dim peptides. Each data point is an average of 10 scans. The peptide concentrations were 5 $\mu$M.

shows the far UV CD spectra of the Cro:2 (the unsubstituted version of CroB:2), CroB:2, CroB:2-dim, and CroB:3-dim (the latter two are the dimeric version of CroB:2 and CroB:3, respectively). The CD spectra of the Cro:2 peptide are characteristic of random coils with no significant intensity around 220 nm and a minimum around 200 nm. CroB:2 on the other hand shows a strong minimum around 220 nm, a characteristic typical of helical peptides. The large change of the 220 nm band upon Aib substitution suggests conversion of a mostly random coil conformation to a helical conformation upon Aib substitution. CroB:2-dim shows spectra similar to that of CroB-2. CroB:3-dim on the other hand has an enhanced negative value of mean residue ellipticity at 220 nm, suggesting that it has higher helical content than CroB:2. This is not surprising since only one Aib residue is on the portion that has been deleted from CroB:2 to generate CroB:3. Proportionately CroB:3 contains more Aib residues and is expected to have a higher helical content. Promotion of helical conformation upon Aib substitution is also supported by NOESY spectra (NH-NH region; Supplementary Figure S1) of CroB:1, which show many cross-peaks that are characteristics of a helical conformation.

The binding affinity of the Cro:1 and CroB:1 monomers were determined. Binding of the Cro:1 monomer with the wild type $O_R3$ was estimated to be weak with a dissociation constant around 25 $\mu$M or above, whereas the corresponding value for the CroB:1 monomer was around 5.3 $\mu$M (data not shown). This indicates some improvement in the binding affinity of the peptide mimic upon stabilization of the helix due to incorporation of Aib residues. Nonspecific binding of the CroB:2 monomer was tested using NMR titration. Supplementary Figure S2 shows the NMR spectra of $O_R3$ and a mutant operator site $O_R3$-c12. The peak shifts are much less in the $O_R3$-c12 spectra, indicating significantly lesser binding. Thus, the constrained monomeric peptide has significant discrimination ability (details of mutant operator sites are given in the next section).

The CroB:2-dim was prepared by cross-linking with bis-maleimido hexane (BMH). The peptide was purified by HPLC, and the mass was confirmed by mass spectrometry (see Methods). Binding isotherm of the CroB:2-dim against $O_R3$ was determined by titrating fluorescein end-labeled $O_R3$ with CroB:2-dim. The binding isotherm was fitted to a single site equation to yield a dissociation constant of 102 ± 35 nM (Figure 3A). The binding was also verified by isothermal titration calorimetry (Supplementary Figure S3). The dissociation constant obtained from the ITC experiment is 124 nM, which compares favorably with the fluorescence anisotropy measurements. The measured dissociation constant is about 50-fold lower than that of the CroB:2 monomer alone. Two factors may be operative here. The dimer binding may be assisted by additional binding energy from the second helix-turn-helix motif and chelate-like entropic assistance[17] but may be opposed by the distortion of protein and DNA structure necessary for binding of the dimer. A similar increase in affinity was obtained by Kajino *et al.* for a stabilized helix.[11]

**CroB:2-dim Binds to All Three Right Operator-Site Sequences with High Affinity.** Wild-type *Cro* binds to the right operator of bacteriophage $\lambda$ with site affinity in the order $O_R3 > O_R1, O_R2$.[18] This order of affinity is presumed to be important for its biological functions, although the structural basis of this selectivity is not entirely clear.[16] CroB:2-dim binds to both $O_R1$ and $O_R2$ with affinity comparable to that of $O_R3$ (Figure 3B and C). DNA sequences and their relative binding affinities are shown in Supplementary Table S1. The value of the extracted dissociation constants were 120 ± 37 and 126 ± 30 nM for $O_R2$ and $O_R1$, respectively. There is virtually no discrimination between the operator sites by the dimeric constrained peptide. In contrast, the binding affinity of the wild-type *Cro* protein for $O_R1$ is almost 1 order of magnitude weaker.[19] Why CroB:2-dim is not able to discriminate between the related natural cognate sequences as does *Cro* is not clear from these experiments. In order to understand the lack of discrimination by CroB:2-dim, we have chosen to study the binding of CroB:2-dim with a mutant operator site. $O_R3$ differs from $O_R1$ by only three base-pairs; all of them are situated in the non-consensus half. These base-pairs are 3′, 5′, and 8′ (prime symbol refers to the base-pairs in the non-consensus half). Takeda *et al.* have reported that out of these three base-pairs, the biggest contribution to the differential effect (as obtained by single base-pair substitution) is made by the 3′ base-pair.[19] We have thus studied the binding of 3′ mutant $O_R3$ with CroB:2-dim. Experiments by Takeda *et al.*[19] were reported for the $O_R1$ background, and we assume that the effect of single base-pair change at this position is same for $O_R3$ as well. The

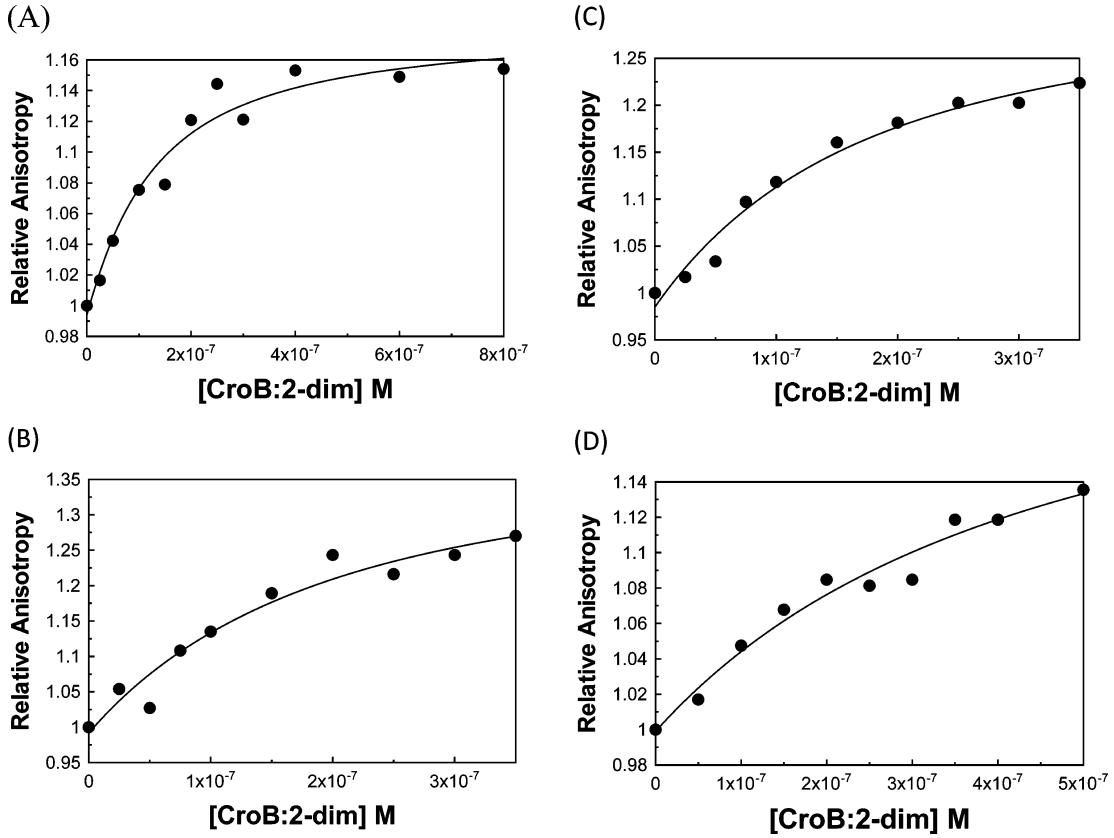


**Figure 3.** Change in anisotropy of four different 5′ fluorescein labeled synthetic duplex oligonucleotides (A) $O_R3$, (B) $O_R1$, (C) $O_R2$, and (D) $O_R3$-r3 with CroB:2-dim. The oligonucleotides were end-labeled with FITC as described in the Methods section. Each point in the figure is an average of six independent titrations.

estimated dissociation constant was 570 ± 117 nM, which is about 6-fold weaker than that for $O_R3$ (Figure 3). Wild-type Cro protein has an approximately 6.3-fold weaker binding affinity with the 3′ substituted mutant $O_R1$ compared to the wild-type $O_R1$.[19] Thus, discrimination of the 3′ base-pair is not the reason behind lack of discrimination of $O_R3$ and $O_R1$ by CroB:2. This point will be further discussed later.

**Peptide Mimics Can Discriminate Individual Base Pairs in the Operator.** Takeda *et al.*[19] have scanned each base-pair of $O_R1$, to which the *Cro* protein binds, to check their contributions to the total binding energy. We have chosen two such mutations to study the specificity of the mimic toward the target DNA sequences. One mutation, c10 (mutation in the 2′ position), reduces the binding by approximately 10-fold, and the other mutation r3 (mutation in the 8 position) has no significant effect on the binding of the wild-type *Cro*.[19] Both are naturally occurring mutations in the phage with distinct phenotypes.[20,21] We have measured binding of CroB:2-dim to oligonucleotides containing the mutant $O_R3$ sequences. As shown in Figure 4, anisotropy increase was $O_R3$-like for fluorescein end-labeled oligonucleotides containing $O_R3$-r3. The dissociation constant was 151 ± 32 nM. There is very little change of affinity compared to the wild-type $O_R3$. This effect is similar to that with the wild-type *Cro*. However, a significant effect was observed in the binding isotherm with $O_R3$-c10. The dissociation constant was estimated to be 449 ± 124 nM. The weakening of binding is comparable to the weakening observed in the *Cro* binding to the same mutant sequences.[19] Thus, with respect to these two base-pairs and to 3′ base-pair discrimination, CroB:2-dim retains the discrimination capability of the native protein.

In order to determine how this *Cro* mimicking peptide binds to unrelated sequences, we have studied binding of CroB:2-dim to four unrelated sequences (Table 1). CroB:2-dim did not bind to a poly dAT sequence up to a concentration of 600 nM. Similarly it has no detectable binding up to 600 nM with a TATA box binding sequence. It binds to a cMyc target site with 17 times lower affinity and to an *E. coli* galactose operon external operator $O_E$ with 12 times lower affinity. To assess whether other potential DNA-binding peptides bind to $O_R3$, we have designed (Supplementary Figure S4) and synthesized a dimeric peptide mimicking a eukaryotic transcription factor cMyc. cMyc is a basic helix−loop−helix leucine zipper class transcription factor, which uses helices as recognition element. We have used a similar strategy as our *Cro* mimic peptide to design and synthesize this dimeric peptide mimic (mass spectra of this construct is shown in Supplementary Figure S5). Table 2 shows the dissociation constants of cMyc peptide with three target binding sites, poly dAT, $O_R3$, and $GalO_E$. This peptide shows no detectable binding to poly dAT and $GalO_E$ and binds to $O_R3$ with an affinity that is many fold lower than that of CroB:2-dim, suggesting nonspecific peptide binding. Thus, cMyc peptide will be used as a control for experiments described below.

**A Smaller Mimic Binds with Even Higher Affinity.** In spite of considerable selectivity of the mimic, the dissociation constant of $O_R3$/CroB:2-dim (about $1 \times 10^{-7}$ M) is still several orders of magnitude lower compared to that of the native Cro-$O_R3$ complex ($4 \times 10^{-12}$ M). One possible difference is that,


dx.doi.org/10.1021/cb200523n | *ACS Chem. Biol.* 2012, 7, 1084−1094

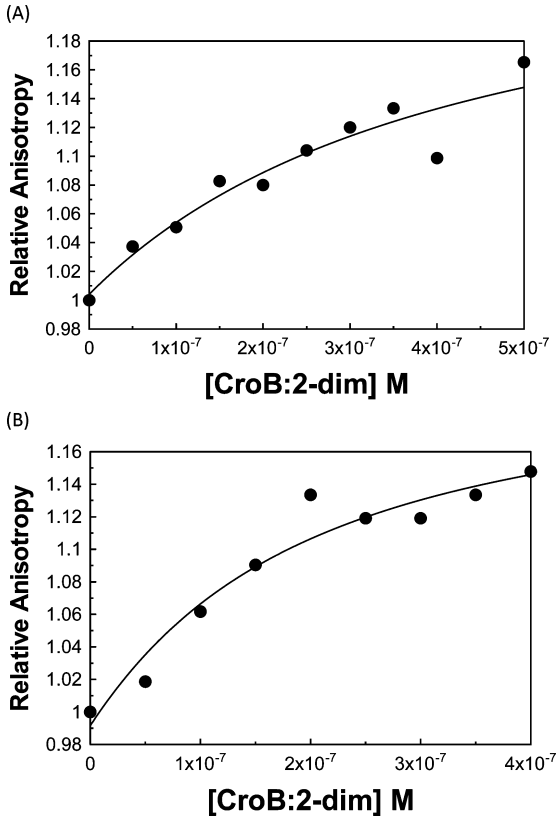


**Figure 4.** Binding isotherms of (A) $O_R3$-c12 and (Bb) $O_R3$-c10 with CroB:2-dim as determined by fluorescence anisotropy. The oligonucleotides were end-labeled with FITC as described in the Methods section. Each point in the figure is an average of six independent titrations.

notwithstanding the stabilization of the helix, the peptide may still retain considerable flexibility, hence requiring sacrifice of some entropy. However, the entire difference may not be due to the entropic factor, as electrostatic interactions between the protein residues outside the chosen region and the nucleic acid occurs. One such interaction is K56, which interacts with a backbone phosphate.

**Table 2. Nonspecific Binding of cMyc-dimer Peptide to Different Target Sites**

| Oligonucleotide | Sequence | $K_d^{DNA}/K_d^{cMyc}$ |
|---|---|---|
| cMyc | 5'-CGAGTAGCACGTGCTACTC-3'<br>3'- CTCATCGTGCACGATGAGC-5' | 1 |
| $O_R3$ | 5'-TATCACCGCAAGGGATA-3'<br>3'-ATAGTGGCGTTCCCT AT-5' | 12.9 |
| dAT | 5'-AAAAATTTATTTTAAATTT-3'<br>3'-TTTTTTAAATAAAATTTAAA-5' | Large; binding not detectable |
| $GalO_E$ | 5'-GCGTGTAAACGATTCCACGC-3'<br>3'-CGCACATTTGCTAAGGTGCG-5' | Large; binding not detectable |

In the Cro-$O_R3$ structure, the primary recognition helix spans residues 26−36. Residues 15−25 only provide additional sugar−phosphate contacts at residues 17 and 18. We argued that residues 15−25 in the peptide (as opposed to that in the whole protein) may not contribute significant binding energy to the complex due to entropic factors and may even be a hindrance. Thus, we engineered a smaller peptide mimic (CroB:3) containing only the recognition helix of the Cro protein (residues 26−36). The CroB:3 peptide was cross-linked with BMH to synthesize the CroB:3-dim. After purification by RP-HPLC, the mass of the peptide dimer was confirmed by mass spectrometry. The binding affinity of the CroB:3-dim was measured by isothermal titration calorimetry. The CroB:3-dim showed an increased binding affinity toward the $O_R3$ operator with a dissociation constant of 10 nM (Figure 5).

**Peptide Mimic CroB:3-dim Interacts with $O_R3$ in the Same Manner as Cro.** Peptide mimics created this way appear to preserve the base specificity indicating native-like interactions. The nature of the protein−DNA interface was studied by chemical shift perturbation experiments of the CroB:3-dim proton resonances with a symmetric operator sequence, sym-$O_R$. A symmetric operator, sym-$O_R$, was chosen as the same operator sequence was used in the crystal structure

**Table 1. Nonspecific Binding of CroB:2-dimer to Selected Oligonucleotides**

| Oligonucleotide | Sequence | $K_d^{DNA}/K_d^{OR3}$ |
|---|---|---|
| $O_R3$ | 5'-TATCACCGCAAGGGATA-3'<br>3'-ATAGTGGCGTTCCCT AT-5' | 1 |
| polydAT | 5'-AAAAATTTATTTTAAATTT-3'<br>3'-TTTTTTAAATAAAATTTAAA-5' | Large; binding not detectable |
| cMyc | 5'-CGAGTAGCACGTGCTACTC-3'<br>3'- CTCATCGTGCACGATGAGC-5' | 17.4 |
| $GalO_E$ | 5'-GCGTGTAAACGATTCCACGC-3'<br>3'-CGCACATTTGCTAAGGTGCG-5' | 12.3 |
| TATA | 5'-CTTATGCAAATGAG-3'<br>3'-GAATACGTTTACTC-5' | Large; binding not detectable |


dx.doi.org/10.1021/cb200523n | ACS Chem. Biol. 2012, 7, 1084−1094

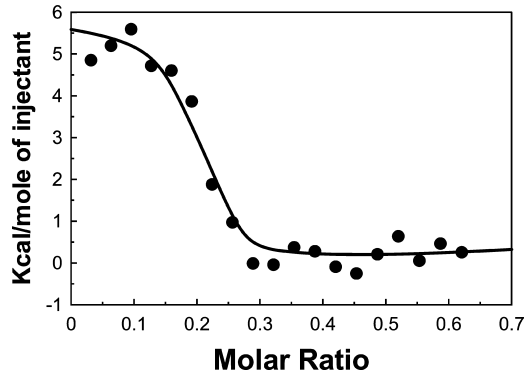


**Figure 5.** Isothermal titration calorimetry of CroB:3-dim with wild type $O_R3$ oligonucleotide. The experiment was carried out at 25 °C. The data were fitted to a single site binding isotherm in Microcal Origin 7.0.

determination, making meaningful comparison with the crystal structure possible.[16] The NMR spectra of the CroB:3-dim show distinct amide peaks, which were assigned by a standard NOESY/TOCSY walk (Supplementary Figure S6). To determine the residues involved in binding with the operator DNA, TOCSY spectra of the CroB:3-dimer with and without sym-$O_R$ DNA were overlaid, and the chemical shift differences were noted. Significant N−H chemical shift changes were observed for Q2, S3, A4, K7, A8, H10, and R12 upon addition of DNA (Supplementary Figure S7 and Figure 6). According to the crystal structure determined by Albright and Matthews[16] in

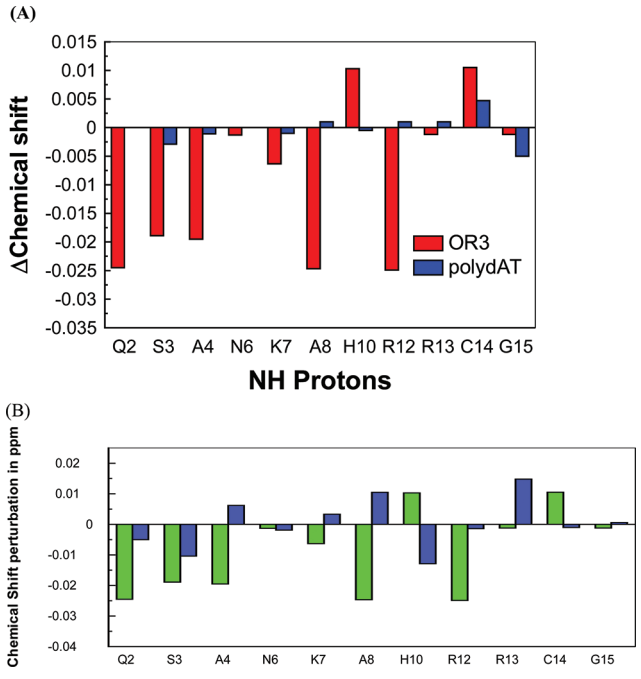


**Figure 6.** Change in chemical shift values of (A) NH protons of the amino acids in the CroB:3-dimer peptide in presence of Sym-$O_R3$ (red) and polydAT (Blue) and (B) alpha (green) and beta protons (blue) of the corresponding amino acids of the CroB:3-dimer peptide upon addition of the Sym-$O_R3$ operator to the CroB:3-dim peptide. All NMR spectra were recorded at 1 mM peptide concentration in 20 mM potassium phosphate buffer, pH 8.0 containing 20 mM KCl and 5% $D_2O$ at 27 °C with and without 100 $\mu$M Sym-$O_R3$ (or polydAT) DNA.

the *Cro* protein with the same symmetric operator, the residues Q2, S3, A4, K7, and H10 (equivalent residues are Q27, S28, A29, K32, and H35 in the *Cro* protein) are all involved in the binding of the DNA, but the chemical shift change of residue N31, which is involved in the Cro−DNA interface according to the crystal structure, falls well below the threshold. This may indicate a small departure in the recognition of the DNA by the designed peptide mimic. To determine the effect of a piece of oligonucleotide of similar size, we have added poly dAT and determined the chemical shift changes (Figure 6a). The chemical shift changes are much smaller, indicating that the detected shifts upon addition of sym-$O_R3$ are due to specific binding of the operator site.

Chemical shift perturbation studies of protons of bases of the symmetric DNA in presence of the CroB:3-dim were also performed. TOCSY and NOESY spectra of the symmetric $O_R$ DNA in $D_2O$ were recorded. Sequential assignments of the 6H/8H protons of the DNA bases were done from the NOESY and TOCSY spectra by standard methods (Supplementary Figure S8).[22] According to the available crystal structure determined by Albright and Matthews[16] the Cro protein contacts all 14 base-pairs of the 17 base-pair $O_R3$ (seven from either end) apart from the middle three bases. The most significant contacts are made at positions A2, G11, G12, and G14 of the operator DNA. The chemical shift perturbation experiments conducted by overlaying the respective NOESY spectra of the DNA and that of the DNA in presence of the CroB:3-dimer also indicate significant chemical shift changes of the A2-T16, C4-G14 and C7-G11 base-pairs (Figure 7). However, the C6-G12 base-pair shows a relatively small chemical shift change. Additionally, A15 shows a large chemical shift change. Reason for this large change is not clear, although this could be a result of a discrimination process of the 3′ base-pair. The middle three base-pairs are not contacted by the wild type *Cro* protein, but a significant conformational change of the DNA is reported on binding with the *Cro* dimer.[23,24] This conformational distortion of the DNA may account for the significant chemical shift changes of the middle cytosine residues. We have also performed a chemical shift perturbation study of the base protons using c-Myc-dim as the control. This dimeric peptide was designed as a DNA-binding peptide modeled on an extant transcription factor c-Myc. The design, synthesis, and characterization of this peptide are given in the Supporting Information. This peptide binds to c-Myc target sequence with good affinity (dissociation constant of 24.7 ± 0.6 nM; Supplementary Figure S9). This compares favorably with the wild-type cMyc-Max and Max-Max binding to their target site.[25] Addition of this peptide to the symmetric $O_R3$-sym causes only small perturbation of chemical shifts of the base protons, the magnitude of which is typically an order of magnitude less than caused by the CroB:3-dim binding. This suggests the observed chemical shift perturbations that occur upon binding to $O_R3$-sym are due to specific recognition of the operator site.

**Peptide Mimic Inhibits Transcription *in Vivo*.** For monitoring the effect of the peptide mimic within an *E. coli* cell, a GFP-based reporter assay was developed. A plasmid construct containing the GFP gene under the control of $\lambda$-$P_R$ promoter was taken (Supplementary Figure S10). The $P_R$ promoter in this construct was regulated by the right operator of phage $\lambda$, which contains $O_R1$, $O_R2$, and $O_R3$ in the natural context.[26] This plasmid was transformed into XL1B cells. The CroB:3-dim was tagged with the cell-permeabilizing peptide $(KFF)_3K$[27]


dx.doi.org/10.1021/cb200523n | *ACS Chem. Biol.* 2012, 7, 1084−1094

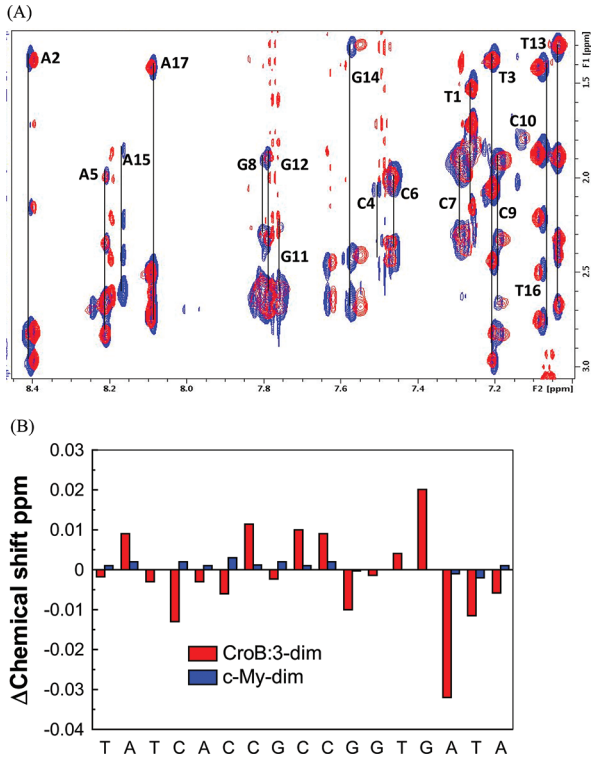


**Figure 7.** Change in chemical shift values of the 6H/8H protons of the corresponding nucleotides of sym-$O_R3$ DNA upon addition. (A) Overlay of the actual spectra. (B) Bar chart of the chemical shift changes upon addition of CroB:3-dim and cMyc-dim peptide. NMR spectra were recorded at 500 $\mu$M DNA concentration in 20 mM potassium phosphate buffer, pH 8.0 in 100% $D_2O$ at 37 °C with and without 50 $\mu$M CroB:3-dimer (or cMyc-dimer) peptide.

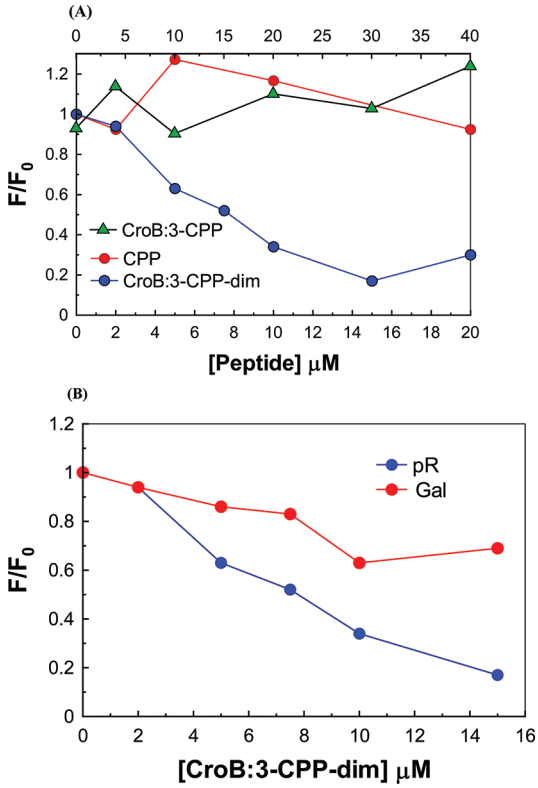


**Figure 8.** Changes in GFP fluorescence upon addition of (A) CPP alone (red), CroB:3-CPP (green), and CroB:3-CPP-dim (blue) into *E. coli* culture containing a GFP expression plasmid under the control of $\lambda$-$P_R$ and $O_R$ regulatory region. CroB:3-CPP was used up to 40 mM as it was a monomer to keep the concentration of the CPP same. (B) Changes in GFP fluorescence upon addition of CroB:3-dim under similar conditions as above when the GFP reporter gene is under control of pR promoter (blue) or Gal promoter (red). Details are given in the Methods section.

to create the CroB:3-CPP-dim, and increasing concentrations of the peptide were added to the bacterial cultures containing the $P_R$-GFP plasmid. This peptide does not significantly affect the growth of *E. coli* (Supplementary Figure S11). After 6 h of growth the cells were centrifuged, the pellet was redissolved in 0.1 M potassium phosphate buffer, pH 7.0, and the $A_{595}$ was measured. Equivalent amounts of cells from each culture were taken, and the GFP levels were monitored. The GFP assay showed that the expression of the GFP gene under the control of the $P_R$ promoter was repressed in a dose-dependent manner due to the addition of the CroB:3-CPP-dim (Figure 8a and Supplementary Figure S12). However, when the CPP alone was added, no repression of GFP levels were seen (Figure 8a). When the monomeric peptide CroB:2-CPP, which has similar amino acid composition but weaker binding, was used, no significant changes were also seen. This indicates that the peptide binds to the $P_R$-promoter region containing the $O_R1$, $O_R2$, $O_R3$ operator sites specifically, resulting in a decreased transcription of the GFP gene. Under normal conditions, *Cro* binds more weakly to $O_R1$, which largely represses $P_R$, than to $O_R3$. Since the mimic binds almost equally well to $O_R1$, it is likely the cause of this repression. The specificity of the peptide was checked by a similar plasmid in which the $O_R$ region is replaced by the *E. coli* gal promoter regulatory region. The repression of the GFP level is significantly weaker (Figure 8b), suggesting that CroB:3-CPP-dim can discriminate different regulatory regions *in vivo*.

To check for the specificity of binding of the designed CroB:3-dim in the whole genome context *in vivo*, a set of whole genome RNA microarray experiments were conducted. The collected raw data were then screened for all expressed genes in *E. coli* for up-regulation or down-regulation with respect to the control cells (those containing no CroB:3-CPP-dim). Results of these experiments show that no genes were up-regulated or down-regulated in a dose-dependent manner. However, a relatively small number of genes were up-regulated and down-regulated in all of the concentrations tested, but not in a dose-dependent manner (Supplementary Table S2). Even assuming that the former set of genes are indeed affected by CroB:3-CPP-dim, the numbers are fairly small. It is probably correct to conclude that CroB:3-CPP-dim does not bind nonspecifically to the genome extensively. The repression of the GFP gene under the control of the lambda $P_R$ promoter due to addition of the mimic into the cell culture and subsequent whole genome RNA microarray experiments reveal that the constrained helical mimic of the *Cro* protein binds specifically to its target gene sequence *in vivo*, without extensive inhibition of nontarget promoters.

**Discussion.** A small synthetic transcription factor may be a very useful tool in cell and tissue engineering as well as in therapeutics. Peptide based mimics may have important advantages over other chemical backbones. Since DNA-binding proteins have evolved in the context of the presence of large amount of other genomic DNA sequences, preserving the core interactions may preserve the sequence specificity of the DNA-


dx.doi.org/10.1021/cb200523n | *ACS Chem. Biol.* 2012, 7, 1084–1094

**Table 3**

| Peptide Name | Peptide Description and Sequence | Expected Mass | Experimental Mass |
|---|---|---|---|
| **Cro:2** | non-Aib 27 mer<br>GQTKTAKDLGVYQSAINKAIHAGRGCG | 2745 | 2745 |
| **CroB:2** | 27-mer with Aib<br>GQTKBAKDLGVYQSABNKABHBGRGCG<br>With cysteine protecting group Acm | 2758 | 2758 |
| **CroB:3** | 15-mer with Aib YQSABNKABHBRRCG | 1716 | 1716 |
| **CroB:3-CPP** | CroB:2 with Cell permeablizing peptide (CPP)<br>KFFKFFKFFKYQSABNKABHBRRCG | 3111 | 3110.5 |
| **CroB:2-dim** | BMH cross-linked CroB:2 dimer through symmetry related cysteines | 5650 | 5650 |
| **CroB:3-dim** | BMH cross-linked CroB:3-dimer through symmetry related cysteines | 3566 | 3567 |
| **CroB:3-CPP-dim** | BMH cross-linked CroB:3-CPP dimer through symmetry related cysteines | 6358 | 6357 |
| **c-Myc-dim** | Branched Aib substituted Myc-Max peptide<br>  | 2807 | 2806 |

binding protein. In addition, proper electrostatic interactions can be incorporated into the peptide based backbone with relative ease as well as protein−protein interaction domains and localization signals.[28] Many years back the usefulness of making synthetic peptide based artificial transcription factors was demonstrated by Kim *et al.* and Weiss *et al.* Kim and co-


dx.doi.org/10.1021/cb200523n | *ACS Chem. Biol.* 2012, 7, 1084−1094

workers synthesized a dimeric disulfide linked peptide version of the transcription factor GCN4. The peptide bound to the target site specifically, but only at 4 °C.[29] However, no detailed quantitative analysis of affinity, specificity, or thermodynamic parameters was reported. Weiss *et al.* produced a truncated version of the protein GCN4 that contained the dimerization and the DNA recognition domain.[30] This truncated protein was able to bind the target sequence with high affinity and specificity like the native protein. In both cases the peptide, which is disordered in solution, became helical upon binding to the target DNA.

Specificity is a key issue in construction of any synthetic transcription factor. Transcription factors must operate in the context of competing sites in the genome as well as in the presence of other transcription factors. In this article we have shown that a cross-linked helical mimic of Cro protein of phage $\lambda$ can bind to the target sequence with a low nanomolar dissociation constant and mimic several single base-pair discriminations of the original protein. However, unlike the whole protein, it is unable to discriminate the two naturally occurring operator sites, $O_R3$ and $O_R1$, to the same extent as the wild-type Cro. The native Cro protein binds to $O_R3$ about 10-fold better than it binds $O_R1$. The peptide mimic binds to $O_R3$ and $O_R1$ with similar affinity. As was stated before, $O_R3$ and $O_R1$ differs by only three base-pairs, at positions 3′, 5′, and 8′ (*i.e.*, in the non-consensus half). The discrimination of $O_R3$ and $O_R1$ by the native Cro is complex and is the sum of several favorable and unfavorable interactions. Interestingly, one of the key base-pairs in the discrimination process, 3′ is well discriminated by the CroB:2-dim to the same extent as the wild-type Cro protein. It appears that discrimination of the two operator sites involves mechanisms that are as yet not completely understood. Further structural analysis is needed to shed light on this important problem.

In contrast to several other approaches to stabilize helices for creation of helix-based synthetic transcription factors, we have chosen substitution of Aib as a strategy for the stabilization of the helix as it minimally changes the sequence and the whole scheme can be easily incorporated into the standard solid phase synthesis strategy. This minimal change may be important for *in vivo* applications as greater modifications create greater chances of undesired interactions. Another novel aspect of the current work is the creation of a two-headed DNA-binding peptide mimic capable of recognizing an inverted repeat. To our knowledge, the only previous example of recognition of DNA sequences by stabilized helices was by monomeric stapled helices. Thus, this synthetic approach allows one to build a peptide mimic that allows one to recognize inverted repeats. Replacement of recognition motif of *Cro* by helical motifs of other repressors may enable one to construct protein mimics that may recognize different nucleotide sequences on DNA. It is also possible to link recognition motifs of two different repressors, thus creating protein mimics that may recognize DNA sequences other than inverted repeats. Incorporation of isosteric amino acids that switches hydrogen bond donors and acceptors within this framework may further expand the library of DNA-binding modules.[31] In conclusion, it appears that single base-pair discrimination capability is achievable by dimeric helical mimics. Due to ease of synthesis and design, incorporation of Aib into recognition helices at suitable positions may offer a good way of creating DNA-binding protein mimics and may allow us to probe the basic principles of biomolecular recognition in complex biological systems as well as provide new reagents for cellular engineering and drug discovery.

## METHODS

All chemical reagents were of ACS grade or higher and purchased from Sigma unless otherwise indicated. All protected amino acids were from Novabiochem (Switzerland). The rest of the chemicals were from either Pierce (USA) or Aldrich (USA). All oligonucleotides were either purchased from Isogen (The Netherlands) with a C6-aminolink at the 5′-end or synthesized in an automated in-house DNA synthesizer using standard phosphoramidite chemistry. The different oligonucleotide sequences used are as given in Supplementary Table S1

**Peptide Synthesis.** The peptide mimics were synthesized in solid phase *via* Fmoc chemistry on Rink amide MBHA resin (for synthesis of the branched c-Myc peptide Rink amide PEGA resin was used) in a peptide synthesizer manufactured by Protein Technologies, Inc. (AZ, USA). The peptides were cleaved from the resin by treatment with a cocktail containing 97.5% TFA, 0.5% water, 0.5% phenol, 0.5% anisole, 0.5% thioanisole, and 0.5% ethanedithiol for 2.5 h followed by precipitation in cold diethyl ether. The precipitate was collected by centrifugation, dried, dissolved in 0.1% TFA water, and purified by RP-HPLC.

**Cross-Linking.** After purifying the peptides with the cysteine protected by Acm, Acm was removed by mercury(II) acetate as described in the "Catalogue & peptide synthesis handbook" (Novabiochem). This was followed by the gel filtration of the reaction mixture in 0.05 M potassium phosphate buffer, pH 6.65. DTNB reaction was performed to confirm the Acm removal.[32] The reaction with the cross-linking agent was performed immediately after this by addition of the cross-linking agent (bis-maleimidohexane) to the peptide in the ratio 1:2 with continuous stirring. Then the reaction mixture was subjected to RP-HPLC to purify the desired dimer product. The reaction mixture was dissolved in $H_2O$ containing 0.1% TFA and was subjected to RP-HPLC in Waters HPLC using 0−60% $CH_3CN/H_2O$ gradient containing 0.1% TFA on a C-18 $\mu$-BONDAPAC reverse phase column. The peaks were monitored at 215 and 280 nm. In all of the cases only major peaks were collected and characterized through $^1$H NMR and mass spectrometry.

**Mass Determination.** Electrospray ionization in positive mode MS was done on an ESI-MS mass spectrometer (Micromass, Waters, USA) or in a ABI-4800 MALDI-TOF-TOF mass spectrometer. The samples were prepared in 50% acetonitrile/50% water containing 0.1% formic acid. Sequences of the peptides synthesized are shown in Table 3 below.

Table 3 shows the sequences of the various peptides that were synthesized and the respective masses (B stands for Aib and Ahx for 6-amino hexanoic acid). Mass numbers are rounded off to nearest integers. A representative example of mass spectra is shown in Supplementary Figure S13. The cMyc-dim peptide was created using a solid phase branching protocol. The chain was grown simultaneously through $\alpha$- and $\epsilon$-amino groups of lysine linked to the solid phase through its carboxyl group. The details of this procedure will be published in the future.

**Chemical Modification.** Oligonucleotides bearing a 5′-C6 amino link were labeled with fluorescein isothiocyanate. The synthetic oligonucleotides were purchased from Isogen, Inc. The oligonucleotides were labeled with FITC in a 500 $\mu$L solution containing 1 M sodium carbonate/bicarbonate buffer, pH 9.0: DMF/water in a ratio of 5:2:3. Reaction was done for 16 h at 25 °C, with continuous stirring. After incubation, the reaction mixture was loaded onto a Sephadex-G25 column and eluted with 0.1 M potassium phosphate buffer, pH 8.0. The oligonucleotide and its complementary strand were annealed by heating at 80 °C for 0.5 h and then cooling slowly to RT.

**Fluorescence Spectroscopy.** All fluorescence studies were done in a Perkin-Elmer LS55 spectrofluorimeter at 25 °C, and the experiments were carried out in a 1 cm path length quartz cuvette. The excitation wavelength was at 480 nm, emission was at 530 nm, and the excitation and emission band passes were 5 nm each. Each of

the samples was taken in 50 mM Tris-HCl buffer, pH 8. The anisotropy values were fitted to the following single site binding equation using Kyplot:.

$$A_{obs} = A_0 + [(A_\infty - A_0)(K_d + X + [DNA]) - \sqrt{(K_d + X + [DNA])^2 - 4X[DNA]}]/2[DNA]$$

where $A_{obs}$ is the observed anisotropy, $A_0$ is the initial anisotropy, $A_\infty$ is the final limiting anisotropy, [DNA] is the fluorescein end-labeled DNA concentration, $X$ is the total peptide concentration, and $K_d$ is the dissociation constant. All concentrations were expressed in molar units.

**Circular Dichroism Spectroscopy.** All CD experiments were done in a JASCO 500 CD spectrometer in 10 mM Tris-HCl, pH 8.0 buffer. Experiments were done in a 1 cm path length quartz cuvette. Averages of 10 independent scans were taken, the control spectrum containing only the buffer was subtracted from the spectra of each peptide to generate the data, and smoothing of the data was done in CD spectra analysis software. The mean residue ellipticity values were generated from the CD (mdeg) curve by correcting for the concentration and the number of residues of the peptide. For ease of comparison only the mean residue ellipticity plots have been shown.

**NMR Spectroscopy.** All $^1$H NMR experiments were performed on a Bruker Avance 600 MHz spectrometer equipped with a cryoprobe. NMR spectroscopy of Cro-1 and CroB:2-dim was performed at a peptide concentration of 1 mM in 20 mM potassium phosphate buffer, pH 7 containing 50 mM KCl and 5% $D_2O$ at 27 °C. Water suppression was achieved by WATERGATE pulse sequence for all experiments. TOCSY and NOESY experiments were performed using standard protocols. The DNA NMR experiments were performed at a DNA concentration of 1 mM in 20 mM potassium phosphate buffer, pH 7 (in 100% $D_2O$) at 27 °C.

Chemical shift perturbation experiments for the Cro B:3 dimer were done by adding 20 $\mu$M (final concentration) of $O_R3$ (or poly dAT) DNA to a 200 $\mu$M peptide solution and repeating the TOCSY experiment done with the peptide previously. For the chemical shift perturbation experiment of the Sym-$O_R3$ DNA 50 $\mu$M (final concentration) of the peptide (Cro B:3 or c-Myc) was added to a 500 $\mu$M DNA solution, and the NOESY experiment was repeated.

**Isothermal Titration Calorimetry.** All ITC experiments were done in a VPITC instrument from Microcal Inc. The titrations were done in 50 mM Tris-HCl buffer, pH 8.0 at 25 °C. The peptide dimer (5 $\mu$M) was taken in the cell (volume 1.47 mL), and the $O_R3$ DNA (50 $\mu$M) was added from a syringe with continuous stirring. The data were fitted to a single site binding isotherm using MS Origin 7.0 software.

**GFP Assay.** For monitoring the effect of the peptide mimic within the cell, a GFP assay was developed. A plasmid construct containing the GFP gene under the control of the $P_R$ promoter was taken. The $P_R$ promoter contains all three operators $O_R1$, $O_R2$, and $O_R3$ to which the *Cro* protein binds.[21] Since the operator-promoter sequence is identical to phage $\lambda$ genome, wild-type Cro is expected to repress $P_R$ in this construct. This plasmid was transformed into XL1B cells. A bacterial cell permeabilizing peptide was attached to the CroB:3 peptide to synthesize the corresponding cell-permeabilizing peptide. Dimerization of this peptide with BMH cross-linker was done in a manner similar to the one described before to produce the CroB:3-CPP-dim. Bacterial cultures of *E. coli* XL1B strain were taken in seven different test tubes. Increasing concentrations of CroB:3-CPP-dim were added to the seven different culture tubes starting from 0 $\mu$M CroB:3-CPP-dim to 20 $\mu$M CroB:3-CPP-dim. The bacterial cultures were then shaken at 37 °C for 6 h. The cell pellets were then collected by centrifugation and dissolved in 1 mL of 0.1 M potassium phosphate buffer, pH 7.0. The absorbance of the respective samples was then measured in a 1 cm path length quartz cuvette. All cells were diluted to an OD of 0.1, and the respective fluorescence was measured in a LS55 Perkin-Elmer spectrofluorometer. As a control an untransformed XL1B cell was grown, and fluorescence intensity of 0.1 OD of the same cells was also recorded. This was then subtracted from all recorded fluorescence intensities. The $F/F_0$ values were then plotted against the peptide concentration for comparing the level of repression of GFP expression in the two cases. The same experiment was repeated on the pR-GFP plasmid with the CroB:3-CPP dimer peptide (which is expected to bind the pR promoter and repress transcription) and the CPP peptide (not expected to bind the pR promoter).

**Toxicity Study.** To check for the effect of the CroB:3-CPP dimer on the growth of *E. coli* cells, a growth curve experiment was done. In six test tubes 6 mL of LB containing 5, 10, and 20 $\mu$M of CroB:3-CPP dimer and CPP control peptide were taken and inoculated with 1% of overnight XL1B culture. The cells were then grown at 37 °C. Samples of volume 500 $\mu$L were collected from each test tube at regular intervals, collected by centrifugation, and dissolved in 500 $\mu$L of 1X PBS buffer. The absorbance of the respective samples was then measured in a Perkin-Elmer UV−vis spectrophotometer and plotted against time to generate the growth curve.

**Whole Genome Microarray Experiments.** To check for the effect of CroB:3-CPP-dim on the *E. coli* genome a whole genome RNA microarray experiment was conducted. The CroB:3-CPP-dim was added to XL1B cell cultures followed by shaking at 37 °C for 6 h. Cells were then collected by centrifugation and dissolved in a RNA later solution. The microarray experiments were conducted by Genotypic, Inc. (Bangalore, India) on payment for service basis. After extraction of the RNA from cells, labeling of the RNA was done. The labeled RNA was then loaded into high quality 60-mer oligonucleotide *in situ* microarray. This was followed by hybridization and overnight incubation of the samples. They were then subjected to a high-throughput scan, and the data were collected and analyzed.

## ■ ASSOCIATED CONTENT

### Ⓢ Supporting Information

This material is available free of charge *via* the Internet at http://pubs.acs.org.

## ■ AUTHOR INFORMATION


### Corresponding Author

*E-mail: sidroykolkata@gmail.com.

### Author Contributions

†These authors contributed equally to this work.


### Notes

The authors declare no competing financial interest.

## ■ ACKNOWLEDGMENTS

We acknowledge research support from Council of Scientific Research (Govt. of India). We also acknowledge Department of Science and Technology (Govt. of India) for J.C. Bose Fellowship to S.R. We also acknowledge O. Kobiler for the GFP plasmid.

## ■ ABBREVIATIONS

Aib, $\alpha$-amino isobutyric acid; BMH, bis-maleimido hexane; CD, circular dichroism; CPP, cell penetrating peptide; DMF, dimethyl formamide; *E. coli*, *Escherichia coli*; FITC, fluorescein isothiocyanate; GFP, green fluorescent protein; HPLC, high performance liquid chromatography; LB, Luria broth; MALDI, matrix assisted laser desorption ionization; NMR, nuclear magnetic resonance; NOESY, nuclear Overhauser effect spectroscopy; PBS, phosphate-buffered saline; TFA, trifluoroacetic acid; TOCSY, total correlation spectroscopy; TOF, time of flight

## ■ REFERENCES

(1) Vazquez, M. E., Caamano, A. M., and Mascarenas, J. L. (2003) From transcription factors to designed sequence-specific DNA-binding peptides. *Chem. Soc. Rev. 32*, 338−349.

(2) Ansari, A. Z., and Mapp, A. K. (2002) Modular design of artificial transcription factors. *Curr. Opin. Chem. Biol. 6*, 765−772.
(3) Dervan, P. B., Doss, R. M., and Marques, M. A. (2005) Programmable DNA binding oligomers for control of transcription. *Curr. Med. Chem. Anticancer Agents 5*, 373−387.
(4) Rodríguez-Martínez, J. A., Peterson-Kaufman, K. J., and Ansari, A. Z. (2010) Small-molecule regulators that mimic transcription factors. *Biochim. Biophys. Acta, Gene Regul. Mech. 1799*, 768−774.
(5) Zondlo, N. J., and Schepartz, A. (1999) Highly specific DNA recognition by a designed miniature protein. *J. Am. Chem. Soc. 121*, 6938−6939.
(6) Majmudar, C. Y., and Mapp, A. K. (2005) Chemical approaches to transcriptional regulation. *Curr. Opin. Chem. Biol. 9*, 467−474.
(7) Brown, R. S. (2005) Zinc finger proteins: getting a grip on RNA. *Curr. Opin. Struct. Biol. 15*, 94−98.
(8) Brennan, R. G., and Matthews, B. W. (1989) The helix-turn-helix DNA binding motif. *J. Biol. Chem. 264*, 1903−1906.
(9) Huffman, J. L., and Brennan, R. G. (2002) Prokaryotic transcription regulators: more than just the helix-turn-helix motif. *Curr. Opin. Struct. Biol. 12*, 98−106.
(10) Enander, K., Dolphin, G. T., and Baltzer, L. (2004) Designed, functionalized helix-loop-helix motifs that bind human carbonic anhydrase II: a new class of synthetic receptor molecules. *J. Am. Chem. Soc. 126*, 4464−4465.
(11) Kajino, M., Fujimoto, K., and Inouye, M. (2011) Side-chain cross-linked short $\alpha$-helices that behave like original proteins in biomacromolecular interactions. *J. Am. Chem. Soc. 133*, 656−659.
(12) Mahalakshmi, R., and Balaram, P. (2006) Non-protein amino acids in the design of secondary structure scaffolds. *Methods Mol. Biol. 340*, 71−94.
(13) Svenningsen, S. L., Costantino, N., Court, D. L., and Adhya, S. (2005) On the role of Cro in lambda prophage induction. *Proc. Natl. Acad. Sci. U.S.A. 102*, 4465−4469.
(14) Ptashne, M., Jeffrey, A., Johnson, A. D., Maurer, R., Meyer, B. J., Pabo, C. O., Roberts, T. M., and Sauer, R. T. (1980) How the lambda repressor and cro work. *Cell 19*, 1−11.
(15) Ohlendorf, D. H., Tronrud, D. E., and Matthews, B. W. (1998) Refined structure of Cro repressor protein from bacteriophage lambda suggests both flexibility and plasticity. *J. Mol. Biol. 280*, 129−136.
(16) Albright, R. A., and Matthews, B. W. (1998) Crystal structure of lambda-Cro bound to a consensus operator at 3.0 A resolution. *J. Mol. Biol. 280*, 137−151.
(17) Berggrun, A., and Sauer, R. T. (2001) Contributions of distinct quaternary contacts to cooperative operator binding by Mnt repressor. *Proc. Natl. Acad. Sci. U.S.A. 98*, 2301.
(18) Johnson, A., Meyer, B. J., and Ptashne, M. (1978) Mechanism of action of the cro protein of bacteriophage lambda. *Proc. Natl. Acad. Sci. U.S.A. 75*, 1783.
(19) Takeda, Y., Sarai, A., and Rivera, V. M. (1989) Analysis of the sequence-specific interactions between Cro repressor and operator DNA by systematic base substitution experiments. *Proc. Natl. Acad. Sci. U.S.A. 86*, 439.
(20) Maurer, R., Meyer, B., and Ptashne, M. (1980) Gene regulation at the right operator (OR) bacteriophage lambda. I. OR3 and autogenous negative control by repressor. *J. Mol. Biol. 139*, 147−161.
(21) Meyer, B. J., Maurer, R., and Ptashne, M. (1980) Gene regulation at the right operator (OR) of bacteriophage lambda. II. OR1, OR2, and OR3: their roles in mediating the effects of repressor and cro. *J. Mol. Biol. 139*, 163−194.
(22) Weiss, M. A., Patel, D. J., Sauer, R. T., and Karplus, M. (1984) 1H-NMR study of the lambda operator site OL1: assignment of the imino and adenine H2 resonances. *Nucleic Acids Res. 12*, 4035−4047.
(23) Torigoe, C., Kidokoro, S., Takimoto, M., Kyogoku, Y., and Wada, A. (1991) Spectroscopic studies on lambda cro protein-DNA interactions. *J. Mol. Biol. 219*, 733−746.
(24) Brennan, R. G., Roderick, S. L., Takeda, Y., and Matthews, B. W. (1990) Protein-DNA conformational changes in the crystal structure of a lambda Cro-operator complex. *Proc. Natl. Acad. Sci. U.S.A. 87*, 8165−8169.
(25) Kiessling, A., Sperl, B., Hollis, A., Eick, D., and Berg, T. (2006) Selective inhibition of c-Myc/Max dimerization and DNA binding by small molecules. *Chem. Biol. 13*, 745−751.
(26) Kobiler, O., Rokney, A., Friedman, N., Stavans, J., and Oppenheim, A. B. (2005) Quantitative kinetic analysis of the bacteriophage $\lambda$ genetic network. *Proc. Natl. Acad. Sci. U.S.A. 102*, 4470.
(27) Eriksson, M., Nielsen, P. E., and Good, L. (2002) Cell permeabilization and uptake of antisense peptide-peptide nucleic acid (PNA) into Escherichia coli. *J. Biol. Chem. 277*, 7144−7147.
(28) Mapp, A. K., Ansari, A. Z., Ptashne, M., and Dervan, P. B. (2000) Activation of gene expression by small molecule transcription factors. *Proc. Natl. Acad. Sci. U.S.A. 97*, 3930−3935.
(29) Talanian, R. V., McKnight, C. J., and Kim, P. S. (1990) Sequence-specific DNA binding by a short peptide dimer. *Science 249*, 769.
(30) Weiss, M. A., Elleberger, T., Wobbe, C. R., Lee, J. P., Harrisoni, S. C., and Struhl, K. (1990) Folding transition in the DNA-binding domain of GCN4 on specific binding to DNA. *Nature 347*, 11.
(31) Maiti, A., and Roy, S. (2005) Switching DNA-binding specificity by unnatural amino acid substitution. *Nucleic Acids Res. 33*, 5896−5903.
(32) Banik, U., Saha, R., Mandal, N. C., Bhattacharyya, B., and Roy, S. (1992) Multiphasic denaturation of the lambda repressor by urea and its implications for the repressor structure. *Eur. J. Biochem. 206*, 15−21.